On the stability of peptide nucleic acid duplexes in the presence of organic solvents

Anjana Sen and Peter E. Nielsen*

Department of Cellular and Molecular Medicine, Faculty of Health Sciences, University of Copenhagen, The Panum Institute, Blegdamsvej 3c, DK-2200 Copenhagen N, Denmark

ABSTRACT

Nucleic acid double helices are stabilized by hydrogen bonding and stacking forces (a combination of hydrophobic, dispersive and electrostatic forces) of the base pairs in the helix. One would predict the hydrogen bonding contributions to increase and the stacking contributions to decrease as the water activity in the medium decreases. Study of nucleobase paired duplexes in the absence of water and ultimately in pure aprotic, non-polar organic solvents is not possible with natural phosphodiester nucleic acids due to the ionic phosphate groups and the associated cations, but could be possible with non-ionic nucleic acid analogues or mimics such as peptide nucleic acids. We now report that peptide nucleic acid (PNA) (in contrast to DNA) duplexes show almost unaffected stability in up to 70% dimethylformamide (DMF) or dioxane, and extrapolation of the data to conditions of 100% organic solvents indicates only minor (or no) destabilization of the PNA duplexes. Our data indicate that stacking forces contribute little if at all to the duplex stability under these conditions. The differences in behaviour between the PNA and the DNA duplexes are attributed to the differences in hydration and counter ion release rather than to the differences in nucleobase interaction. These results support the possibility of having stable nucleobase paired double helices in organic solvents.

INTRODUCTION

Nucleic acid double helices are stabilized by hydrogen bonding and stacking forces (a combination of hydrophobic, dispersive and electrostatic forces) of the base pairs in the helix (1–5). The most recent data suggest that stacking interactions are the more important for DNA duplex stability (6,7). Indeed these results suggest that while hydrogen bonding in GC base pairs are stabilizing the helix, hydrogen bonding in AT base pairs are slightly destabilizing (6,7). One would predict the hydrogen bonding contributions to increase and the stacking contributions to decrease as the water activity in the medium decreases. Therefore, it could be of great interest both from a structural and thermodynamic as well as from a functional point of view to study nucleobase paired duplexes in the absence of water and ultimately in pure aprotic, non-polar organic solvents.

This is not possible with natural phosphodiester nucleic acids due to the ionic phosphate groups and the associated cations, but could be possible with uncharged nucleic acid analogues or mimics such as methylphosphonates (8), phosphotriesters (9), morpholino derivatives (10) and peptide nucleic acids (PNAs) (11,12). PNAs are DNA pseudopeptide mimics capable of forming DNA-like Watson–Crick base-pair double helices with sequence complementary DNA, RNA and PNA oligomers (13–18). As the aminoethyl glycine backbone of PNA is charge neutral, no counter ions are required for stabilizing PNA·PNA duplexes, and consequently such duplexes may more conveniently be studied in organic solvents.

Results from a previous study has given preliminary indications that PNA–PNA duplexes are much less affected by the presence of organic co-solvent (50% DMF) than DNA–DNA duplexes, correlating well with the lack of measurable changes in hydration or counter ion binding upon PNA duplex formation (19). However, this observation warrants further exploration. We now report that PNA (in contrast to DNA) duplexes show almost unaffected stability in 70% dimethylformamide (DMF) or dioxane, and extrapolation of the data to conditions of 100% organic solvents indicates only a little (or no) destabilization of the PNA duplexes.

MATERIALS AND METHODS

PNAs

PNA1, PNA2, PNA3, PNA4 and PNA5 were synthesized using solid phase Boc chemistry, purified by HPLC and characterized by MALDI-TOF mass spectrometry as described previously (20). PNA concentrations

*To whom correspondence should be addressed. Tel: +45 35 327762; Fax: +45 35 396042; Email: pen@imbg.ku.dk

were determined spectrophotometrically at 65°C using molar extinction coefficients: ε_{260} of adenine = $15\,400\,M^{-1}\,cm^{-1}$, ε_{260} of guanine = $11\,700\,M^{-1}\,cm^{-1}$, ε_{260} of thymine = $8800\,M^{-1}\,cm^{-1}$ and ε_{260} of cytosine = $7400\,M^{-1}\,cm^{-1}$.

Chemicals and DNAs

All chemical reagents used were of analytical grade except for dimethylformamide (DMF) and dioxane, which were spectroscopic grade from Sigma-Aldrich, Munich, Germany. The DNA oligonucleotides were purchased from DNA Technology, Aarhus, Denmark, and used without further purification.

Sample preparation

Main stock solutions of PNAs and DNAs were prepared by dissolution in deionized, double distilled water. Experimental samples were made by diluting from the corresponding main stock solutions in 10 mM phosphate buffer (pH 7.2) containing 100 mM NaCl and 0.1 mM EDTA.

Equimolar mixtures (1:1 stoichiometry in single strands) of the PNA or DNA and its complementary strand were dissolved in the buffer mentioned above with desired amount of organic co-solvents. The duplex formation was assured by heating to 90°C and then cooling slowly to room temperature to allow proper annealing. No sign of aggregation or decreased solubility of the PNAs at up to 70% of organic co-solvents was observed.

UV-melting experiments

The thermal melting experiments were performed on a Cary 300 Bio UV-visible spectrophotometer (Varian, Cary, NC, USA) connected to a temperature controller. Thermal melting profiles were obtained using heating–cooling cycles in the range of −3 to 95°C. The melting temperature (T_m) was determined from the peak of the first derivative of the heating curve. Cuvettes of 1.0 cm path length and 1.0 ml volume were used for all experiments.

Thermal melting curves at >50% of DMF or dioxane start to lose the upper baseline and show severe disturbances partly because of high absorbance of DMF at the wavelength required for the experiments. Therefore, thermodynamic data at >50% of DMF could not be obtained. However, it was possible to obtain T_m values at 60 and 70% of DMF or dioxane.

Thermodynamics

The thermodynamic parameters viz enthalpy change (ΔH^0), entropy change (ΔS^0), and Gibbs' free energy change (ΔG^0) were evaluated using the 'hyperchromicity method' (curve fitting) and/or the concentration method (21).

The hyperchromicity method

The hyperchromicity method utilizes alpha curve and van't Hoff plots (ln K_T versus T^{-1}) according to the following definitions (21): The fraction (α_T) of single strands that remained hybridized in the duplex at a particular temperature T in Kelvin is represented as

$$\alpha_T = \frac{A_s - A}{A_s - A_d} \quad\quad 1$$

where, A_d is the absorbance of the duplex in fully hybridized condition, A_s is the absorbance of the single strands in fully denatured condition and A_s is absorbance at a particular point on the thermal melting curve at temperature T.

For non-self-complementary sequences forming n-mer structures, the general equilibrium constant equation at a particular temperature T can be expressed as:

$$K_T = \frac{\alpha_T}{(1 - \alpha_T)^n (c_{ts}/n)^{n-1}} \quad\quad 2$$

where, c_{ts} represents the total concentration of strands and n is the molecularity of the complex. Assuming a two-state model, Equation (2) reduces to

$$K_T = \frac{2\alpha_T}{(1 - \alpha_T)^2 c_{ts}} \qu\quad 3$$

The van't Hoff plot ln K_T versus T^{-1} is a straight line represented by

$$\ln K_T = \left(-\frac{\Delta H^0}{R}\right)\frac{1}{T} + \left(\frac{\Delta S^0}{R}\right) \qu\quad 4$$

Hence, ΔH^0 can be obtained from the slope and ΔS^0 can be obtained from the Y-intercept of the van't Hoff plot. ΔG^0 at a particular temperature T in Kelvin can be calculated from

$$\Delta G^0 = -RT \ln K_T = \Delta H^0 - T\Delta S^0 \qu\quad 5$$

where R is the universal gas constant which is equal to 1.986 cal/mol K.

The concentration method

The concentration method utilizes a plot of T_m^{-1} versus ln c_{ts}, where T_m is the thermal melting temperature of the duplex and c_{ts} is the total strand concentration of PNA or DNA.

Since T_m is defined by the temperature where $\alpha = 0.5$ for a two state transition, combining Equations (3) and (4) yields:

$$\frac{1}{T_m} = \frac{R}{\Delta H^0}\ln c_{ts} + \frac{\Delta S^0 - R\ln 4}{\Delta H^0}. \qu\quad 6$$

Thus, the thermodynamic parameters can be extracted from a linear fit to a plot of T_m^{-1} versus ln c_{ts} according to Equation (6) (21), where ΔH^0 is obtained from the slope of the linear fit and ΔS^0 from the Y-intercept.

The values of the thermodynamic parameters calculated by this method are thus independent of strand concentration, which is not the case with the hyperchromicity method described above.

RESULTS

PNA and DNA duplexes

In order to elucidate the properties of PNA duplexes as compared to those of iso-sequential DNA duplexes at reduced water activity, we have studied the effect of organic co-solvents on the thermal stability and thermodynamics of PNA·PNA, PNA·DNA and DNA·DNA duplexes of 'random', mixed base-sequence (Table S1). We chose DMF (dielectric constant of DMF is 36.7) and dioxane (dielectric constant of dioxane is 2.2) as organic co-solvents, as these are aprotic and are not hydrogen bond donors but still sufficiently polar to retain solubility of the PNA·DNA complexes even above 50% organic solvent.

The thermal stability of these duplexes and the corresponding thermodynamic parameters [evaluated using both the concentration method (T_m^{-1} versus ln c_{ts} plot) (21) and the hyperchromicity (curve fitting) method (21)] in aqueous medium with increasing amount of DMF (extrapolated to 100% DMF) are presented in Tables 1 and S2. Representative thermal melting curves are shown in Figures S1 and S2. It is important to note that thermal denaturation curves showed essentially unperturbed monophasic behaviour up to 50% organic co-solvent. The extrapolation was performed on the basis of the linear plots of the thermal stability (T_m) and Gibbs' free energy changes (ΔG^0) as a function of increasing amount of DMF in the medium (Figure 1A and B). Because of insufficient thermal stability of the DNA1·DNA2 duplex in >30% DMF, we also designed a longer DNA·DNA duplex (DNA3·DNA4), that has thermal stability in aqueous solution similar to that of the PNA1·PNA2 duplex (data in Tables 1 and S3, Figure 1A and B, representative thermal curves in Figure S3). While the organic solvent-dependent changes in ΔG^0 of all these duplexes show a very good correlation with the corresponding T_m, ΔH^0 and ΔS^0 values were not significantly affected within experimental error (Tables S2–S4). The extraction of thermodynamic parameters derived from thermal melting method requires that no change in heat capacity occurs in the duplex single-strand equilibrium. For the present systems we have found only

Table 1. Thermal stability and thermodynamic parameters of PNA and DNA duplexes[a]

Duplex	DMF[b] (%)	T_m (°C)[c,d]	ΔG^0_{37} (kcal/mol)[d,e]	$\Delta\Delta G^0$ [f]
PNA1·PNA2	0	70.2 ± 0.3	−16.6 ± 0.5 (−17.2)	5.6
	10	68.3 ± 0.2	−15.4 ± 0.5 (−16.2)	
	20	66.2 ± 0.2	−14.3 ± 0.4 (−15.6)	
	30	64.3 ± 0.5	−14.5 ± 0.8 (−15.7)	
	40	63.4 ± 0.3	−14.4 ± 0.5 (−15.9)	
	50	61.3 ± 0.4	−13.6 ± 0.7 (−15.5)	
	60	60.0 ± 0.6[g]	[h]	
	70	56.1 ± 0.5[g]	[h]	
	100[i]	52.6	−11.0	
DNA1·DNA2	0	35.8 ± 0.5	−8.2 ± 0.7 (−7.9)	15.0
	10	29.2 ± 0.4	−6.2 ± 1.2 (−6.1)	
	20	23.7 ± 0.5	−4.9 ± 0.8 (−4.9)	
	30[j]	18.2 ± 0.3	−3.7 ± 0.5 (−3.9)	
	100[i]	−22.9	6.8	
DNA3·DNA4	0	70.0 ± 0.4	−16.4 ± 0.4	19.2
	10	62.1 ± 0.5	−14.3 ± 0.7	
	20	56.2 ± 0.6	−12.8 ± 0.8	
	30	49.2 ± 0.3	−11.3 ± 1.0	
	40	41.3 ± 0.2	−9.3 ± 0.6	
	50	30.1 ± 0.5	−6.1 ± 0.5	
	100[i]	−6.2	2.8	
PNA1·DNA2	0	51.3 ± 0.4	−10.3 ± 1.0	6.8
	10	47.0 ± 0.5	−9.5 ± 0.7	
	20	43.1 ± 0.3	−9.0 ± 0.6	
	30	40.2 ± 0.4	−8.3 ± 0.6	
	40	36.2 ± 0.5	−7.7 ± 0.8	
	50	31.1 ± 0.2	−6.7 ± 0.5	
	100[i]	12.3	−3.5	

[a]PNA and DNA sequences: H-GTA GAT CAC T-Lys-NH$_2$ (PNA1); H-AGT GAT CTA C-Lys-NH$_2$ (PNA2); 5′-GTA GAT CAC T-3′ (DNA1); 5′-AGT GAT CTA C-3′ (DNA2); 5′-AGT GAT CTA CGG TGG ACG GTC C-3′ (DNA3); 5′-GGA CCG TCC ACC GTA GAT CAC T-3′ (DNA4).
[b]Vol% in 10 mM phosphate buffer containing 100 mM NaCl and 0.1 mM EDTA, pH 7.2 ± 0.01.
[c]Duplex concentrations of 5.0 µM in strands were used (T_m plots are in Figures 1A, S4A and S5A).
[d]Standard deviations are based on five independent measurements.
[e]Evaluated from the hyperchromicity (curve fitting) method (21) at 37°C (ΔG^0_{37} plots are in Figures 1B, S4B and S5B). Values obtained from the concentration method (21) (Equation 6) are shown in paratheses (full details of these data are in Supplementary Data).
[f]$\Delta\Delta G^0 = \Delta G^0_{37}$ (DMF) − ΔG^0_{37} (aqueous). Calculated only with the values obtained from the hyperchromicity method.
[g]These data have poorer accuracy due to upper baseline irregularities.
[h]Data could not be evaluated because of bad thermal curves.
[i]Data were obtained from manual extrapolation of the linear plots in Figure 1A and B.
[j]Data obtained at higher than 30% of DMF were not reliable because of too low values of T_m.
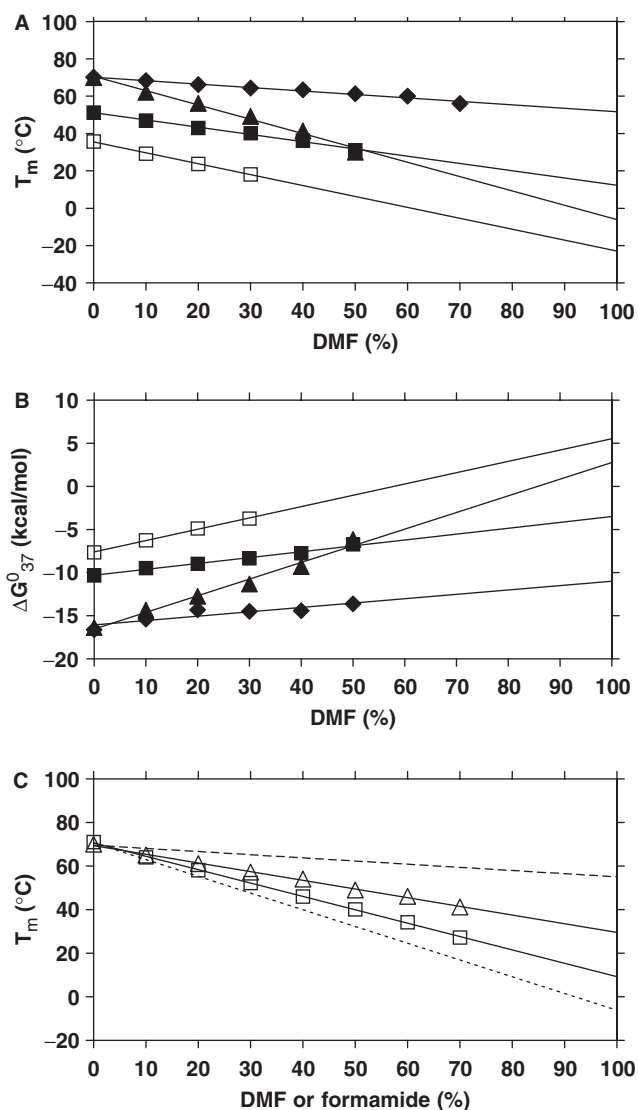
Figure 1. Plots of (**A**) T_m and (**B**) ΔG^0 of PNA1·PNA2 (*solid diamond*), PNA1·DNA2 (*solid square*), DNA1·DNA2 (*open square*) and DNA3·DNA4 (*solid triangle*) as a function of the amount of DMF in the medium. (**C**) Plots of T_m of PNA1·PNA2 (*open triangle*) and DNA3·DNA4 (*open square*), as a function of the amount of formamide in the medium, compared to that of PNA1·PNA2 (dashed line) and DNA3·DNA4 (dotted line), as a function of the amount of DMF in the medium (DMF data taken from Figure 1A). The aqueous buffer was 10 mM phosphate buffer containing 100 mM NaCl and 0.1 mM EDTA, pH 7.2 ± 0.01 (data in Tables 1, S2–S5).

minor changes. The values of specific heat capacity change (enthalpic) at constant pressure (ΔC_p) were 2.0 kcal/mol.K for PNA1·PNA2, 1.4 kcal/mol.K for PNA1·DNA2, 1.9 kcal/mol.K for PNA2·DNA1 and 1.8 kcal/mol.K for DNA1·DNA2 (19).

It is clearly evident that the presence of DMF has a much smaller effect on the thermal stability and free energy of the PNA·PNA duplex than on the DNA·DNA duplex, whereas the effect on the PNA·DNA duplex is intermediate. The plots in Figure 1A and B show a linear dependence of both T_m and ΔG^0 on the DMF concentration. The change in thermal stabilities as a function of the

amount of DMF in the medium did not deviate within experimental error from linearity up to 70% of DMF, thereby supporting a hypothetical approximation beyond 70% of DMF (and an extrapolation of the data to 100% DMF) (Figure 1A and B, Table 1). These results strongly indicate that PNA·PNA duplexes in contrast to DNA·DNA (and PNA·DNA) duplexes will have appreciable stability even in the absence of water. Naturally, we cannot exclude that non-linearity might occur at very low water contents.

Analogous studies of PNA1·PNA2, PNA1·DNA2 and DNA3·DNA4 in dioxane show that, despite the significant difference between the dielectric constants of these solvents, there is no significant difference between the effects of DMF and dioxane on T_m and ΔG^0 (Tables S3 and S4, representative thermal curves in Figures S2 and S3, plots in Figures S4 and S5).

PNA and DNA duplexes in formamide

In order to compare the effect of aprotic solvent (DMF and dioxane, where the destabilization of the duplex is assumed to be predominantly caused by dehydration (and perhaps change in dielectrics) with that of a hydrogen-bond donor (and breaking) solvent, we studied the thermal and thermodynamic properties of PNA1·PNA2 and DNA3·DNA4 in formamide (dielectric constant of formamide is 109), which is a well-established nucleic acid denaturant (Table S5, representative thermal curves in Figure S6, plots in Figures 1C, S7 and S8). In formamide, the destabilization is caused by a combined effect of H-bond disruption and dehydration. Notably, the destabilizing effect of formamide is almost as pronounced for the PNA duplex as for the DNA duplex. The slopes of the linear plots of T_m of PNA1·PNA2 and DNA3·DNA4 as a function of increasing amount of DMF in the medium are -0.17 (without taking the values at 60 and 70% into account) and -0.77, respectively, whereas, those values in formamide are -0.40 and -0.61, respectively (Figure 1C). On the other hand, the decrease in T_m is paralleled by the increases in both ΔG^0 and ΔH^0. Thus in stark contrast to the effects of DMF and dioxane, formamide has comparable effects on PNA and DNA duplex stabilities.

Self-complementary PNA and DNA hairpins

Additionally, we examined the effect of organic co-solvent on the stability of self-complementary (foldback) PNA hairpins (Figure 2). Unfolding of hairpin PNAs, H-AGAG-(eg1)$_3$-CTCT-Lys-NH$_2$ (PNA3) and H-ACAG-(eg1)$_3$-CTGT-Lys-NH$_2$ (PNA4) also showed little change in T_m and ΔG^0 with increasing amount of DMF or dioxane in the medium (Tables S6 and S7, Figures 2A, B and S9). In fact, the hairpins were slightly stabilized in dioxane (Table S7 and Figure 2B), and in this case the stabilization appears to be enthalpic (Table S7). Similar studies with an analogous DNA hairpin (DNA5: 5′-AGAGTTTTCTCT-3′) in DMF and dioxane as a control showed a dramatic thermal destabilization by both co-solvents (Tables S8 and S9, Figures 2C, D and S10).
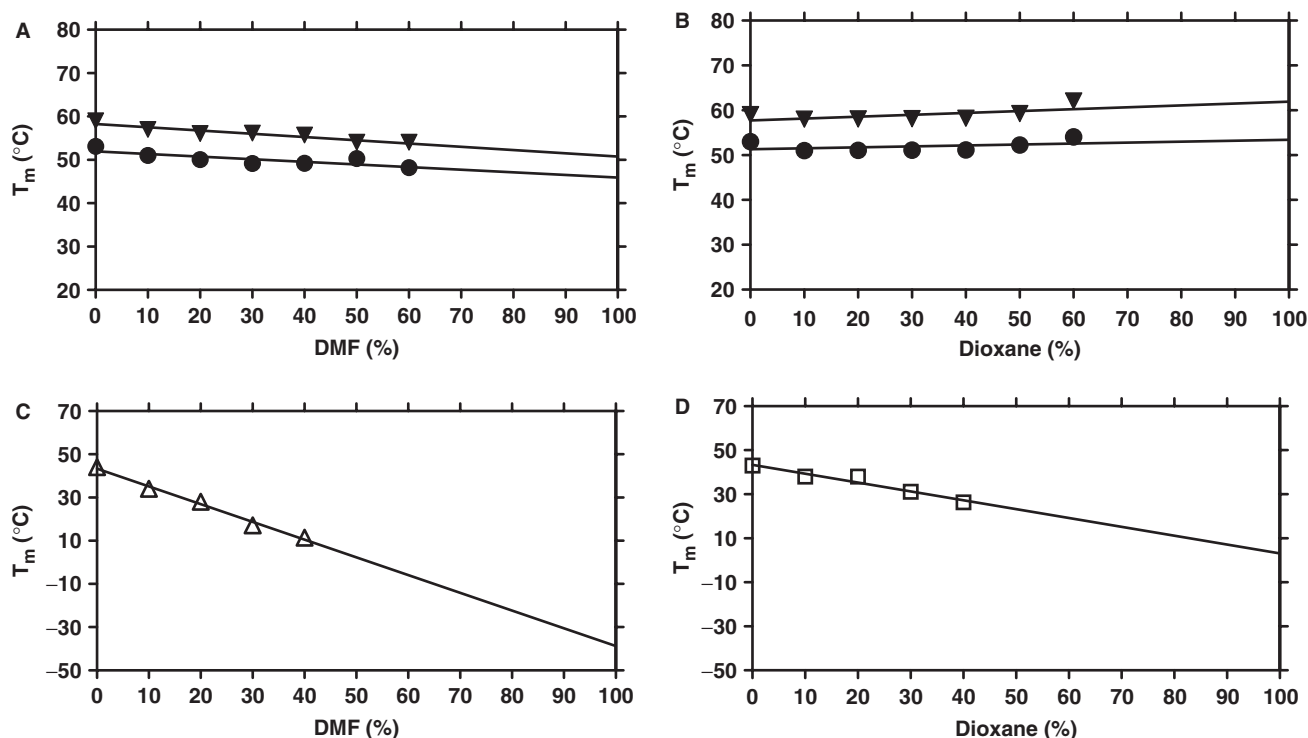
Figure 2. Plots of T_m of self-complementary (hairpin) PNAs PNA3 (*solid inverted triangle*) and PNA4 (*solid circle*) as a function of the amount of (**A**) DMF and (**B**) dioxane in the medium. Plots of T_m of hairpin DNA control DNA5 as a function of the amount of (**C**) DMF (*open triangle*) and (**D**) dioxane (*open square*) in the medium. The aqueous buffer was 10 mM phosphate buffer containing 100 mM NaCl and 0.1 mM EDTA, pH 7.2 ± 0.01 (PNA3: H-AGAG-(eg1)$_3$-CTCT-Lys-NH$_2$, PNA4: H-ACAG-(eg1)$_3$-CTGT-Lys-NH$_2$, DNA5: 5′-AGA GTT TTC TCT-3′) (data in Tables S6–S9).

PNA duplex with an endstacked tricyclic thymine

In order to evaluate the effect of removal of water from the medium (by increasing DMF content) on base stacking forces more directly, we studied the effect of DMF on the behaviour of a PNA duplex (PNA5·PNA6) containing a tricyclic thymine analogue (benzo[*b*]-1,8-naphthyridin-2(1*H*)-one, designated as tT) (22) attached at the end of one strand, thereby stabilizing the duplex predominantly (or entirely) by end-stacking (22). It is evident that, DMF preferentially destabilizes the PNA5·PNA6 duplex (T_m slope is -0.24) compared to the control PNA6·PNA7 duplex (T_m slope is -0.15) (Table S10, Figures 3 and S11). Most interestingly, the stabilization of the duplex contributed by the tT base is completely lost at 70% DMF (Figure 3), clearly indicating a dramatic reduction of the contribution of stacking interactions to duplex stability under these conditions (decrease in thermal stability of PNA5·PNA6 at 70% DMF with respect to 0% DMF, $\Delta T_m = 18.8$, whereas, that of the control duplex PNA6·PNA7 is only 10.7).

Mismatched duplexes

Sequence discrimination is critically dependent on hydrogen bonding recognition, but base-pair mismatches may also change the geometry of the helix and thus influence stacking interactions. For instance, X-ray crystallography and NMR studies have revealed that G·T and
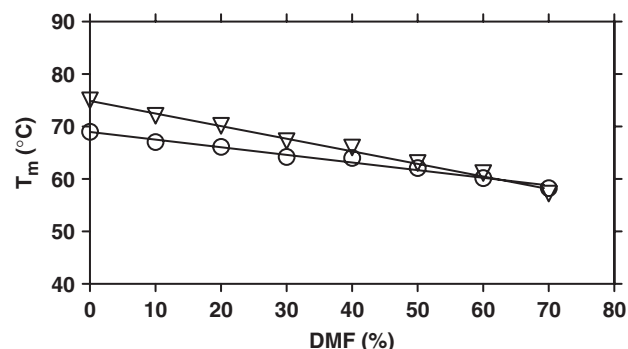

Figure 3. Plots of T_m of PNA5·PNA6 (*open inverted triangle*) containing tricyclic thymine (tT) and its control PNA6·PNA7 (*open circle*), as a function of the amount of DMF in the medium (data in Table S10). The aqueous buffer was 10 mM phosphate buffer containing 100 mM NaCl and 0.1 mM EDTA, pH 7.2 ± 0.01 (PNA5: H-tT-GTA GAT CAC T-NH$_2$, PNA6: H-AGT GAT CTA C-NH$_2$, PNA7: H-GTA GAT CAC T-NH$_2$).

T·T mismatches in DNA likely form wobble base pairs (23–30). The homopurine A·A mismatch in DNA involves one hydrogen bond between the amino group of one adenine and the nitrogen N1 of the opposite adenine, whereas, the mispaired T·T bases in DNA involve two imino-carbonyl hydrogen bonds (23–30). A C·T mismatch is the most unstable in DNA and makes one regular

H-bond involving carbonyl groups along with one weak H-bond bridged by a water molecule at neutral pH (23–30). Effects of mispairs are rather localized and the duplex retains a global B-form conformation (23–30). As hydration and stacking forces could be more important factors for mismatch stabilization, removal of water may preferentially destabilize these.

However, surprisingly we find that the relative effects of DMF on the stability of single base mismatched (T·T, A·A and C·T) duplexes of PNA8 (H-AGT GTT CTA C-Lys-NH$_2$), PNA9 (H-GTA GAA CAC T-Lys-NH$_2$) and PNA10 (H-GTA GCT CAC T-Lys-NH$_2$) with PNA1 and PNA2 are not distinguishable within experimental error from that observed with the corresponding fully matched PNA duplexes (The T_m slope of the fully matched PNA1·PNA2 is −0.17, of T·T mismatched PNA1·PNA8 is −0.13, of A·A mismatched PNA2·PNA9 is −0.08, and of C·T mismatched PNA2·PNA10 is −0.12) (Tables 1 and S11, Figures 1A, 4, S12 and S13). These results suggest that, in these base pair mismatched duplexes, hydrogen bonding and stacking interactions are equally compromised or that the mismatched base pair contributes only very little to the overall duplex stability.

DISCUSSIONS AND CONCLUSIONS

The relative insensitivity of PNA duplexes to the reduced water content is consistent with our previous observations showing that in contrast to the case of DNA·DNA (and to a lesser extent PNA·DNA duplexes), no change in hydration occurs upon duplex formation (19) and no change in counter ion binding is observed either (19).

Thus the effect of organic solvents on PNA duplex stability may be ascribed to changes in base-pair hydrogen bonding and stacking forces of the base pairs. Stacking forces have contributions from hydrophobic, dispersion and dipole electrostatic forces (31–33), and therefore both hydrogen bonding as well as stacking interactions are affected by the dielectric constant of the solvent. However, we observe no correlation between PNA duplex stability and solvent dielectric constant. Water, formamide, DMF and dioxane have dielectric constants of 78, 109, 37 and 2.2, respectively, and in particular the comparable effect of dioxane and DMF strongly argue against a simple dependence of the dielectric constant. On the other hand, it is clear that the contribution of hydrogen bonding to PNA duplex stability should significantly increase when the dielectric constant and especially the hydrogen bonding donor/acceptor activity of the solvent decreases.
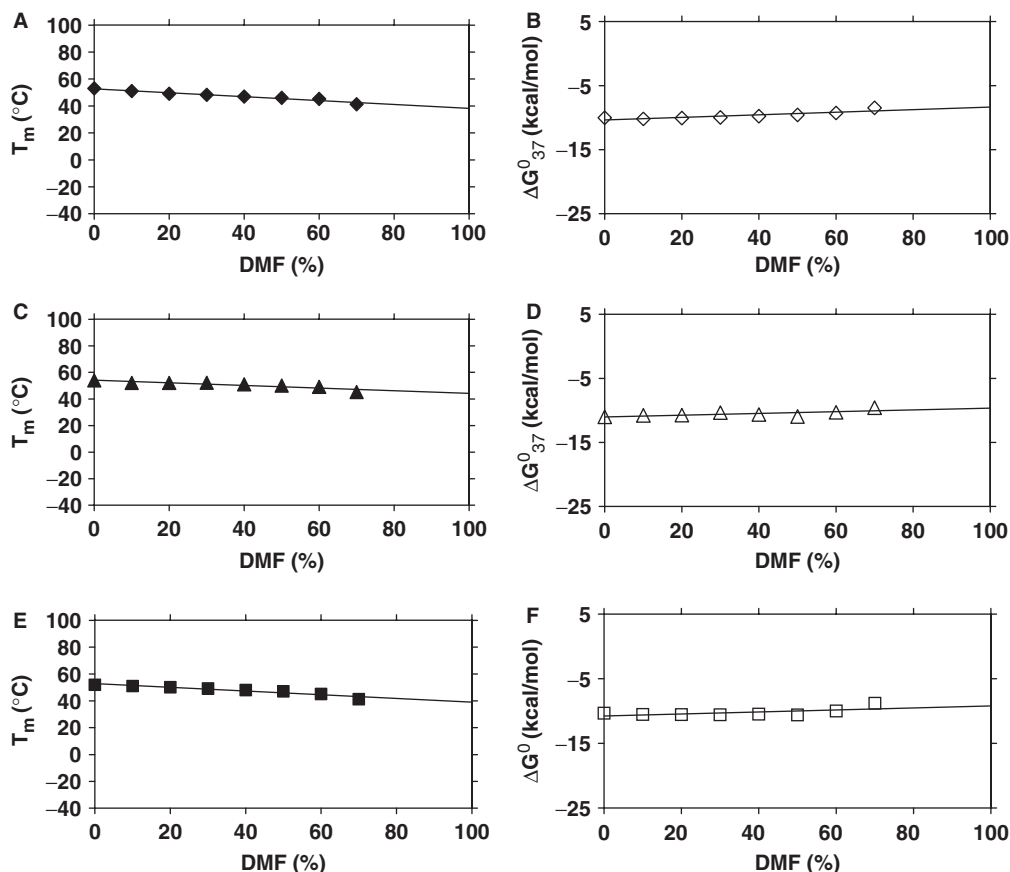

Figure 4. Thermal stabilities of T·T, A·A and C·T mismatched PNA duplexes in DMF (data in Table S11). Plots of (**A**) T_m (*solid diamond*) and (**B**) $\triangle G^0$ (*open diamond*) of PNA1·PNA8 as a function of the amount of DMF in the medium. Plots of (**C**) T_m (*solid triangle*) and (**D**) $\triangle G^0$ (*open triangle*) of PNA2·PNA9 as a function of the amount of DMF in the medium. Plots of (**E**) T_m (*solid square*) and (**F**) $\triangle G^0$ (*open square*) of PNA2·PNA10 as a function of the amount of DMF in the medium. The aqueous buffer was 10 mM phosphate buffer containing 100 mM NaCl and 0.1 mM EDTA, pH 7.2 ± 0.01.

(It should be kept in mind that the hydrogen bond stabilization results as the difference between nucleobase hydrogen bonding to solvent versus base pairing.) Furthermore, our results very clearly show that the stabilizing effect of end stacking decreases upon addition of DMF to the solvent. Indeed, the end-stacking effect using a tricyclic thymine analogue is absent already at 70% DMF. This thymine analogue in essence contains an additional phenyl ring compared to thymine (22), and therefore the stacking interactions of the tricyclic thymine are expected to contain a relatively larger hydrophobic contribution than natural nucleobase pairs (32). Thus a similar effect on the natural nucleobases is expected to occur at higher DMF (lower water) content. Nonetheless, our results strongly support the contention that relative helix stabilizing contribution of base-pair hydrogen bonding and base stacking will be shifting towards hydrogen bonding as the water content of the medium (as well as the dielectric constant) decreases. In this context, we note that for the PNA hairpins an increased stability is indicated with increasing concentration of the low dielectric constant solvent dioxane (in contrast to DMF).

It is well established that formamide and urea destabilize DNA and RNA duplexes (34,35), and in agreement with the present data, the effect of DMF and dioxane (at 10 mol%) on RNA duplex stability was found to be comparable to that of formamide (33). However, also in case of RNA, no direct correlation between the duplex stabilizing effect and the solvent dielectric constant was apparent (33). Indeed, from our data comparing the effects of formamide and DMF on PNA duplex stability, we would argue that the effects of organic solvents on DNA and RNA duplexes is to a larger extent due to hydration (solvation) and counterion effects, whereas the effects on PNA duplexes more directly reflect changes in hydrogen bonding and stacking contributions to helix stability. Thus more systematic studies on the different behaviour of PNA versus DNA duplexes could possibly shed light on these relative contributions to nucleobase (including DNA) helix stability.

Interestingly, the data (Tables S2 and S3) could hint that the decreased stability of the DNA duplexes upon removal of water appears to be primarily entropic rather than enthalpic, though the data are not conclusive. This would be compatible with the differences in behaviour between the PNA and the DNA duplexes (as mentioned above) being caused by the differences in hydration and counter ion release rather than via nucleobase interaction. Thus, these results can be of great significance in understanding nucleobase pairing systems, and it will be of great interest to learn whether other non-ionic DNA analogues such as methylphosphonates (8), phosphotriester (9) and morpholino (10) derivatives behave similarly.

The possibility of having stable nucleobase paired double helices in organic solvents has several implications. First of all, we note that it should be possible to reach the goal of finding PNA duplexes that are freely soluble in non-polar organic solvents by chemically modifying the PNA backbone, for instance using hydrophobic amino acids in place of glycine (36). Studying the behaviour of these in the absence of water could provide valuable information about fundamental properties of nucleobase double helices. Furthermore, PNA duplexes spanning lipid membranes could be envisaged as a means for mediating electron transport over the membrane. Sequence-dependent electron transport (or hole migration) through DNA duplexes is now well established (37–41), and although electron transport involving PNA still require more extensive studies (42,43) this should be worthwhile pursuing. Finally, entirely new dimensions would be added to the emerging technique of 'DNA sequence' directed organic synthesis (44). Thus novel avenues of exploiting nucleobase recognition systems can be enabled by transferring these to non-aqueous environments.

SUPPLEMENTARY DATA

Supplementary data are available at NAR Online.

REFERENCES

1. Watson,J.D. and Crick,F.H. (1953) Genetical implications of the structure of deoxyribonucleic acid. *Nature*, **171**, 964–967.
2. Saenger,W. (1988) *Principles of Nucleic acid Structure*. Springer, New York.
3. Kool,E.T. (2001) Hydrogen bonding, base stacking, and steric effects in DNA replication. *Annu. Rev. Biophys. Biomol. Struct.*, **30**, 1–22.
4. Oostenbrink,C. and van Gunsteren,W.F. (2005) Efficient calculation of many stacking and pairing free energies in DNA from a few molecular dynamics simulations. *Chemistry*, **11**, 4340–4348.
5. Sundaralingam,M. and Ponnuswamy,P.K. (2004) Stability of DNA duplexes with Watson–Crick base pairs: a predicted model. *Biochemistry*, **43**, 16467–16476.
6. Protozanove,E., Yakovchuk,P. and Frank-Kamenetskii,M.D. (2004) Stacked-unstacked equilibrium at the nick site of DNA. *J. Mol. Biol.*, **342**, 775–785.
7. Yakovchuk,P., Protozanove,E. and Frank-Kamenetskii,M.D. (2006) Base-stacking and base-pairing contributions into thermal stability of the DNA double helix. *Nucleic. Acids Res.*, **34**, 564–574.
8. Miller,P.S, Yano,J., Yano,E., Carroll,C., Jayaraman,K. and Ts'o,P.O. (1979) Nonionic nucleic acid analogues. Synthesis and characterization of dideoxyribonucleoside methylphosphonates. *Biochemistry*, **18**, 5134–5143.
9. Tosquellas,G., Alvarez,K., Dell'Aquila,C., Morvan,F., Vasseur,J-J., Imbach,J-L. and Rayner,B. (1998) The pro-oligonucleotide approach: solid phase synthesis and preliminary evaluation of model pro-dodecathymidylates. *Nucleic Acids Res.*, **26**, 2069–2074.
10. Summerton,J. (1999) Morpholino antisense oligomers: the case for an RNase H-independent structural type. *Biochim. Biophys. Acta*, **1489**, 141–158.
11. Nielsen,P.E., Egholm,M., Berg,R.H. and Buchardt,O. (1991) Sequence-selective recognition of DNA by strand displacement with a thymine-substituted polyamide. *Science*, **254**, 1497–1500.
12. Nielsen,P.E. (1999) Peptide nucleic acid. A molecule with two identities. *Acc. Chem. Res.*, **32**, 624–630.

13. Egholm,M., Buchardt,O., Christensen,L., Behrens,C., Freier,S.M., Driver,D.A. *et al.* (1993) PNA hybridizes to complementary oligonucleotides obeying the Watson–Crick hydrogen-bonding rules. *Nature*, **365**, 566–568.

14. Wittung,P., Nielsen,P.E., Buchardt,O., Egholm,M. and Nordén,B. (1994) DNA-like double helix formed by peptide nucleic acid. *Nature*, **368**, 561–563.

15. Jensen,K.K., Ørum,H., Nielsen,P.E. and Nordén,B. (1997) Kinetics for hybridization of peptide nucleic acids (PNA) with DNA and RNA studied with the BIAcore technique. *Biochemistry*, **36**, 5072–5077.

16. Brown,S.C., Thomson,S.A., Veal,J.M. and Davis,D.G. (1994) NMR solution structure of a peptide nucleic acid complexed with RNA. *Science*, **265**, 777–780.

17. Eriksson,M. and Nielsen,P.E. (1996) Solution structure of a peptide nucleic acid-DNA duplex. *Nature Struct. Biol.*, **3**, 410–413.

18. Rasmussen,H., Kastrup,J.S., Nielsen,J.N., Nielsen,J.M. and Nielsen,P.E. (1997) Crystal structure of a peptide nucleic acid (PNA) duplex at 1.7 Å resolution. *Nature Struct. Biol.*, **4**, 98–101.

19. Sen,A. and Nielsen,P.E. (2006) Unique properties of purine/pyrimidine asymmetric PNA.DNA duplexes: differential stabilization of PNA.DNA duplexes by purines in the PNA strand. *Biophys. J.*, **90**, 1329–1337.

20. Christensen,L., Fitzpatrick,R., Gildea,B., Petersen,K., Hansen,H.F., Koch,T., Egholm,M., Buchardt,O., Nielsen,P.E. *et al.* (1995) Solid-phase synthesis of peptide nucleic acids. *J. Pept. Sci.*, **1**, 175–183.

21. Peyret,N., Seneviratne,P.A., Allawi,H.T. and SantaLucia,J.Jr (1999) Nearest-neighbor thermodynamics and NMR of DNA sequences with internal A.A, C.C, G.G, and T.T mismatches. *Biochemistry*, **38**, 3468–3477.

22. Eldrup,A., Nielsen,B.B., Haaima,G., Rasmussen,H., Kastrup,J.S., Christensen,C. and Nielsen,P.E. (2001) 1,8-Naphthyridin-2(1*H*)-ones—novel bicyclic and tricyclic analogues of thymine in peptide nucleic acids (PNAs). *Eur. J. Org. Chem.*, **9**, 1781–1790.

23. Patel,D.J., Shapiro,L. and Hare,D. (1987). In Eckstein,F. and Lilley,D.M.J. (eds), *In Nucleic acid and Molecular Biology*. Springer, Berlin, pp. 70–84.

24. Germann,M.W., Kalisch,B.W., Varnum,J.M., Vogel,H.J. and van de Sande,J.H. (1998) NMR spectroscopic and enzymatic studies of DNA hairpins containing mismatches in the EcoRI recognition site. *Biochem. Cell Biol.*, **76**, 391–402.

25. Allawi,H.T. and SantaLucia,J.Jr (1998) Thermodynamics of internal C.T mismatches in DNA. *Nucleic. Acids Res.*, **26**, 2694–2701.

26. Boulard,Y., Cognet,J.A.H. and Fazakerley,G.V. (1997) Solution structure as a function of pH of two central mismatches, C.T and C.C, in the 29 to 39 K-ras gene sequence, by nuclear magnetic resonance and molecular dynamics. *J. Mol. Biol.*, **268**, 331–347.

27. Nemecek,D., Stepanek,J., Turpin,P.Y. and Rosenberg,I. (2004) Raman study of potential 'antisense' drugs: nonamer oligonucleotide duplexes with a central mismatch as a model system for the binding selectivity evaluation. *Biopolymers*, **74**, 115–119.

28. Hunter,W.N., Brown,T., Kneale,G., Anand,N.N., Rabinovich,D. and Kennard,O. (1987) The structure of guanosine-thymidine mismatches in B-DNA at 2.5-Å resolution. *J. Biol. Chem.*, **262**, 9962–9970.

29. Ke,S.-H. and Wartell,R.M. (1996) The thermal stability of DNA fragments with tandem mismatches at a d(CXYG).d(CY′X′G) site. *Nucleic. Acids Res.*, **24**, 707–712.

30. Gervais,V., Cognet,J.A., Le Bret,M.L., Sowers,C. and Fazakerley,G.V. (1995) Solution structure of two mismatches A.A and T.T in the K-ras gene context by nuclear magnetic resonance and molecular dynamics. *Eur. J. Biochem.*, **228**, 279–290.

31. Guckian,K.M., Schweitzer,B.A., Ren,R.X-F., Sheils,C.J., Tahmassebi,D.C. and Kool,E.T. (2000) Factors contributing to aromatic stacking in water: Evaluation in the context of DNA. *J. Am. Chem. Soc.*, **122**, 2213–2222.

32. Kim,T.W. and Kool,E.T. (2005) A series of nonpolar thymidine analogs of increasing size: DNA base pairing and stacking properties. *J. Org. Chem.*, **70**, 2048–2053.

33. Hickey,D.R. and Turner,D.H. (1985) Solvent effects on the stability of A_7U_7p. *Biochemistry*, **24**, 2086–2094.

34. Hutton,J.R. (1977) Renaturation kinetics and thermal stability of DNA in aqueous solutions of formamide and urea. *Nucleic. Acids Res.*, **4**, 3537–3555.

35. Blake,R.D. and Delcourt,S.G. (1996) Thermodynamic effects of formamide on DNA stability. *Nucleic. Acids Res.*, **24**, 2095–2103.

36. Püschl,A., Sforza,S., Haaima,G., Dahl,O. and Nielsen,P.E. (1998) Peptide nucleic acids (PNAs) with a functional backbone. *Tetrahedron Lett.*, **39**, 4707–4710.

37. Schuster,G.B. (2004) *In Long-Range Charge Transfer in DNA I-II.* Springer, Heidelberg.

38. Delaney,S. and Barton,J.K. (2003) Long-range DNA charge transport. *J. Org. Chem.*, **68**, 6475–6483.

39. Fink,H.W. and Schonenberger,C. (1999) Electrical conduction through DNA molecules. *Nature*, **398**, 407–410.

40. Wan,C., Fiebig,T., Schiemann,O., Barton,J.K. and Zewail,A.H. (2000) Femtosecond direct observation of charge transfer between bases in DNA. *Proc. Natl Acad. Sci. USA*, **97**, 14052–14055.

41. Shao,F., Augustyn,K. and Barton,J.K. (2005) Sequence dependence of charge transport through DNA domains. *J. Am. Chem. Soc.*, **127**, 17445–17452.

42. Armitage,B., Ly,D., Koch,T., Frydenlund,H., Orum,H., Batz,H.G. and Schuster,G.B. (1997) Peptide nucleic acid-DNA duplexes: long range hole migration from an internally linked anthraquinone. *Proc. Natl Acad. Sci. USA*, **94**, 12320–12325.

43. Tanabe,K., Yoshida,K., Dohno,C., Okamoto,A. and Saito,I. (2000) Control of electron transfer in DNA by peptide nucleic acids (PNA). *Nucleic Acids Symp. Ser.*, **44**, 35–36.

44. Gertner,Z.J., Tse,B.N., Grubina,R., Doyon,J.B., Snyder,T.M. and Liu,D.R. (2004) DNA-templated organic synthesis and selection of a library of macrocycles. *Science*, **305**, 1601–1605.